

1 Long- and short-read metabarcoding technologies reveal
2 similar spatio-temporal structures in fungal communities

3 Brendan Furneaux^{1,*}, Mohammad Bahram^{2,3}, Anna Rosling⁴,
4 Nourou S. Yorou⁵, Martin Ryberg¹

5 ¹Program in Systematic Biology, Department of Organismal Biology,
6 Uppsala University, Uppsala, Sweden

7 ²Department of Ecology, Swedish University of Agricultural Sciences,
8 Uppsala, Sweden

9 ³Institute of Ecology and Earth Sciences, University of Tartu, Tartu, Estonia

10 ⁴Program in Evolutionary Biology, Department of Ecology and Genetics,
11 Uppsala University, Uppsala, Sweden

12 ⁵Research Unit in Tropical Mycology and Plant-Fungi Interactions, LEB,
13 University of Parakou, Parakou, Benin

14 *Corresponding author, brendan.furneaux@ebc.uu.se

Abstract

Fungi form diverse communities and play essential roles in many terrestrial ecosystems, yet there are methodological challenges in taxonomic and phylogenetic placement of fungi from environmental sequences. To address such challenges we investigated spatio-temporal structure of a fungal community using soil metabarcoding with four different sequencing strategies: short amplicon sequencing of the ITS2 region (300–400 bp) with Illumina MiSeq, Ion Torrent Ion S5, and PacBio RS II, as well as long amplicon sequencing of the full ITS and partial LSU regions (1200–1600 bp) with PacBio RS II. Resulting community structure and diversity depended more on statistical method than sequencing technology. The use of long-amplicon sequencing enables construction of a phylogenetic tree from metabarcoding reads, which facilitates taxonomic identification of sequences. However, long reads present issues for denoising algorithms in diverse communities. We present a solution that splits the reads into shorter homologous regions prior to denoising, and then reconstructs the full denoised reads. In the choice between short and long amplicons, we suggest a hybrid approach using short amplicons for sampling breadth and depth, and long amplicons to characterize the local species pool for improved identification and phylogenetic analyses.

1 Introduction

Fungi are key drivers of nutrient cycling in terrestrial ecosystems. One important guild of fungi form ectomycorrhizas (ECM), a symbiosis between fungi and plants in which fungal hyphae enclose the plant’s fine root tips. The fungi provide nutrients and protection from pathogens in exchange for carbon from the plant (Smith & Read, 2010). Approximately 8% of described fungal species are thought to take part in ECM symbiosis (Ainsworth, 2008; Rinaldi et al., 2008). Although only about 2% of land plant species form ECM, these include

38 ecologically and economically important stand-forming trees belonging to both temperate and
39 boreal groups such as Pinaceae and Fagaceae, and tropical groups such as Dipterocarpaceae,
40 *Uapaca* (Phyllanthaceae) and Fabaceae tr. Amherstieae (Brundrett, 2017).

41 Although ECM fungi form many well-known mushrooms (e.g., *Amanita*, *Cantharellus*, *Bo-*
42 *letus*), some instead produce inconspicuous (e.g., *Tomentella*) or no (e.g., *Cenococcum*) fruit
43 bodies. Even when fruitbodies are large, they are ephemeral, so study of ECM communi-
44 ties is facilitated by looking at vegetative structures (Horton & Bruns, 2001). Unlike many
45 saprotrophic fungi which grow easily in axenic culture, ECM fungi are usually difficult to
46 culture, so DNA barcoding is increasingly used to investigate vegetative structures in the
47 field. The advent of high-throughput sequencing (HTS) has facilitated such studies by pro-
48 viding enough sequencing depth for metabarcoding of bulk environmental samples such as
49 soils (Lindahl et al., 2013).

50 As additional techniques and methods are developed for HTS, there is an increasing array
51 of choices for researchers investigating fungal communities. Fungal metabarcoding studies
52 using short-read HTS technologies have targeted the ITS1 or ITS2 regions, which provide
53 sufficient resolution to distinguish fungal species in many groups, and which are usually short
54 enough for HTS (Lindahl et al., 2013; Schoch et al., 2012). The resulting sequencing reads
55 are clustered by sequence similarity to form operational taxonomic units (OTUs), which are
56 then used as the units for further community analysis (Lindahl et al., 2013). If taxonomic
57 identification is desired in order to put OTUs in a wider context and associate functional
58 information, it has usually been performed by database searches using BLAST (Altschul et al.,
59 1990; Lindahl et al., 2013). However, this approach comes with some potential weaknesses.

60 While ITS1 and ITS2 often have suitable variation to distinguish species, they cannot be
61 reliably aligned over the fungal kingdom (Lindahl et al., 2013; Tedersoo, Tooming-Klunderud,
62 et al., 2018). Additionally, the wide range of length variation of these regions may introduce

63 bias in recovery of different taxa. Further bias is introduced by variation in the 5.8S region
64 which separates the two ITS regions, as well as in the 5' end of LSU, which makes it difficult
65 to design primers that are suitable for all fungi (Tedersoo et al., 2015).

66 Distance-based clustering conflates intra-species variation and sequencing error, and results
67 are dataset-specific. In contrast, more recent denoising methods such as DADA2 (Callahan
68 et al., 2017), Deblur (Amir et al., 2017), and UNOISE2 (Edgar, 2016b) utilize read quality
69 information to control for sequencing error while preserving intra-species variation. The
70 resulting units are known as amplicon sequence variants (ASVs) or exact sequence variants
71 (ESVs), as they should represent true amplicon sequences from the sample. Unlike cluster-
72 based OTUs, ASVs can capture variation of as little as one base pair, and are less dataset
73 specific (Callahan et al., 2017).

74 Assignment of taxonomic identities using BLAST requires *a priori* choice of thresholds for
75 different taxonomic ranks. Several algorithms specifically designed for taxonomic assignment
76 have been published which use information about variability within different taxa in the
77 reference database to assign unknown sequences, along with confidence estimates for these
78 assignments (e.g., Wang et al., 2007; Edgar, 2016a; Murali et al., 2018a). In addition,
79 methods have been published which integrate predictions from multiple algorithms to increase
80 the reliability of assignments (Gdanetz et al., 2017; Somervuo et al., 2016).

81 Recent long-read HTS technologies such as Pacific Biosciences Single Molecule Real Time
82 sequencing (PacBio) enable sequencing longer amplicons which include both the ITS re-
83 gions and the flanking, more highly conserved SSU and/or LSU regions (Tedersoo, Tooming-
84 Klunderud, et al., 2018). This can potentially improve taxonomic placement of sequences that
85 lack close database matches and allow the alignment of metabarcoding reads for subsequent
86 phylogenetic analysis. Information from phylogenetic trees produced from long-amplicon
87 metabarcoding has the potential to both improve taxonomic assignment and provide al-

88 ternative measures of community alpha and beta diversity. Because OTU clustering may
89 both “clump” different species into a single OTU, and “split” a single species into multiple
90 OTUs (Ryberg, 2015), diversity measures based on counting species within a community or
91 shared species between two communities may give different results depending on the cluster-
92 ing threshold. In contrast, phylogenetic community distance measures (Wong et al., 2016)
93 are relatively insensitive to species/OTU delimitation, but require a phylogenetic tree. Phy-
94 logenetic placement algorithms have been developed to place short amplicon reads onto a
95 reference tree (Berger et al., 2011; Matsen et al., 2010), but are not easy to apply to ITS
96 sequences because they require that the query sequences be aligned to a reference alignment.
97 Additionally, methods exist to place OTUs on a simplified tree based on taxonomic assign-
98 ments (Tedersoo, Sánchez-Ramírez, et al., 2018). However, long amplicon sequencing allows
99 the inclusion of alignable regions for construction of more fully resolved phylogenetic trees
100 directly from metabarcoding reads. However, long-read technologies are currently more ex-
101 pensive per read compared to short-read sequencing, and so their use entails a trade-off with
102 sequencing depth and/or sample number (Kennedy et al., 2018).

103 Here we investigated the effects of different sequencing strategies and post-analysis on bi-
104 ological conclusions using measurement of the spatiotemporal turnover rate of the fungal
105 community in an ECM-dominated Soudanian woodland in Benin by metabarcoding of bulk
106 soil, sampled at narrow intervals, over two years. We compare three different sequencing
107 platforms (PacBio RS II, Illumina MiSeq, Ion Torrent Ion S5), long and short amplicons,
108 three different taxonomic assignment algorithms (RDP classifier, SINTAX, IDTAXA) and
109 reference databases (Unite, Warcup, RDP), and two different community distance measures
110 (Bray-Curtis vs. weighted UNIFRAC). We also present new algorithms for dividing the rDNA
111 into regions, combining denoising results from multiple regions, and incorporating phyloge-
112 netic information into taxonomic assignments.

2 Materials and Methods

2.1 Sampling

Sampling was conducted at two sites (Ang: N 9.75456° W 2.14064°; Gan: N 9.75678° W 2.31058 °) approximately 30 km apart in the *Forêt Classée de l’Ouémé Supérieur* (Upper Ouémé Forest Reserve) in central Benin. Both sites were located in woodlands dominated by the ECM host tree *Isobertinia doka* (Caesalpinioideae). At each site, 25 soil samples were collected along a linear transect at intervals of 1 m in May 2015. One third of the sample locations (3 m spacing) were resampled one year later in June 2016. For each sample, any coarse organic debris was removed from the soil surface and a sample of approximately 5cm×5cm×5cm was extracted with a sterilized knife blade. Each sample was sealed in a plastic zipper bag and homogenized by shaking and manually breaking apart soil aggregations. Approximately 50 mg total of soil was collected from two locations in the homogenized soil sample and placed into a separate 2.0 mL microtube containing 750 µL of lysis buffer and lysis beads (Xpedition™ Soil/Fecal DNA miniprep, Zymo Research Corporation, Irvine, California, USA) and lysed in the field using a handheld bead-beater (TerraLyser™; Zymo Research Corporation).

An additional sample was collected at every sampling location (1-m spacing) in 2016 using LifeGuard™ Soil Preservation Solution (MO BIO, Carlsbad, CA; USA) for preservation, without field lysis. Sequencing results for these samples differed significantly (PERMANOVA with 9999 permutations, $p < 0.0001$, $R^2 = 0.06$) from samples preserved using the Xpedition™ lysis buffer (Figures S1, S2, and S3); as such these samples were excluded from our spatial analyses. However, reads from these samples were included in the full bioinformatics workflow, including ASV calling, OTU clustering, and phylogenetic trees.

2.2 DNA extraction, amplification, and sequencing

After field lysis, DNA was extracted using the Xpedition™ Soil/Fecal Prep kit (see above). Samples preserved using LifeGuard were first centrifuged at 10000 g for 1 minute, after which the supernatant was removed and DNA was extracted from the remaining soil using the Soil/Fecal Prep kit as for the other samples. DNA was quantified using fluorometrically using Quant-iT™ PicoGreen™ dsDNA (Thermo Fisher Scientific, Waltham, MA, USA) fluorescent indicator dye on a Infinite F200 plate spectrofluorometer (Tecan Trading AG, Männedorf, Switzerland) according to the manufacturer's protocol.

Two different fragments of the nuclear rDNA were amplified (Figure S4). The short amplicon (approximately 300 bp) targeted the full ITS2 region as well as parts of the flanking 5.8S and large subunit (LSU) rDNA, using gITS7 (Ihrmark et al., 2012) as the forward primer and a mix of ITS4 (White et al., 1990) and ITS4a (Urbina et al., 2016) as the reverse primer (hereafter, ITS4m). The long amplicon (approximately 1500 bp) targeted the full ITS region including the 5.8S rDNA and approximately 950 bp at the 5' end of the LSU, including the first three variable regions (Figure S4), using ITS1 (White et al., 1990) as the forward primer and LR5 (Vilgalys & Hester, 1990) as the reverse primer. Each PCR run also included a blank sample and a positive control consisting of freshly extracted DNA from a commercially purchased fruitbody of *Agaricus bisporus*.

The gITS7 primers for the short amplicon were indexed for multiplexing (Supplementary File 1). Amplification was performed by polymerase chain reaction (PCR) in 20µl reactions containing 200 µM dNTP mix, 250 µM indexed gITS7 primer, 150µM ITS4m, 2mM MgCl₂, 0.1 U *Taq* polymerase (Dream *Taq*, Thermo Fisher Scientific, Waltham, MA, USA) and 3–7 ng purified DNA in Dream *Taq* buffer. The reaction conditions were 10 min at 95°, followed by 35 cycles of 60 s at 95°, 45 s at 56°, and 50 s at 72°, and finally 3 min at 72°. Each reaction was conducted in three technical replicates to reduce the effect of PCR

161 stochasticity, which were pooled after amplification.

162 Both primers for the long amplicon were indexed for multiplexing (Supplementary File 2).
163 PCR was performed as for the short amplicons, but with 500 μ M of each of the two primers.
164 Reaction conditions were 10 min at 95°, 30 cycles of 45 s at 95°, 45 s at 59°, and 90 s at 72°,
165 and finally 10 min at 72°. Each reaction was performed in three technical replicates as for
166 short amplicons.

167 Amplicons were purified using SPRI beads (Vesterinen et al., 2016) and quantified fluoromet-
168 rically as above. An aliquot of 100 ng of DNA from each sample (or the total PCR product
169 if less than 100 ng) was pooled into two libraries each for long and short amplicons. Each
170 library was sequenced using Single Molecule Real Time (SMRT) sequencing on a Pacific Bio-
171 sciences (PacBio) RS II sequencer at the Uppsala Genome Center (UGC; Uppsala Genome
172 Center, Science for Life Laboratory, Dept. of Immunology, Genetics and Pathology, Uppsala
173 University, BMC, Box 815, SE-752 37 UPPSALA, Sweden). Short amplicon libraries were
174 sequenced on two SMRT cells each, while long amplicon libraries were sequenced on four
175 SMRT cells each.

176 Additionally, the short amplicon libraries were combined and sequenced using an Ion S5 (Ion
177 Torrent) sequencer using one 520 chip at UGC, and a MiSeq (Illumina Inc.) sequencer using
178 v3 chemistry with a paired-end read length of 300 bp at the SNP&SEQ Technology Platform
179 (Dept. of Medical Sciences, Uppsala University, BMC, Box 1432, SE-751 44 UPPSALA,
180 Sweden). The Illumina library was pooled with samples for another project, with half of the
181 reads from one lane devoted to the current study.

182 **2.3 Bioinformatics**

183 Circular consensus sequence (CCS) basecalls for PacBio sequences were made using `ccs`
184 version 3.4 (Pacific Biosciences, 2016, July 13/2019) using the default settings. The resulting

185 sequences, as well as the paired-end Illumina sequences, were demultiplexed and sequencing
186 primers were removed using `cutadapt` version 2.8 (Martin, 2011). Sequencing primers were
187 similarly removed from the Ion Torrent sequences, but interference between the tagged gITS7
188 primers and the Ion XPress tags used in library prep made full demultiplexing of the Ion
189 Torrent sequences impossible, and these reads were thus only analyzed as a pool. For Ion
190 Torrent and PacBio, reads were discarded if they did not have the appropriate primers on
191 both ends. Reads were searched in both directions, and reads where the primers were found
192 in the reverse direction were reverse complemented before further analysis. For Illumina
193 sequences, read pairs were only retained when PCR primers were detected at the 5' ends
194 of both the forward and reverse read. Primers were also searched for and removed on the
195 3' ends of the reads, in case of readthrough with short amplicons. Read pairs where the
196 primers were found in reverse orientation were kept in separate files, but were retained in
197 their original orientation until after denoising.

198 **2.3.1 Denoising**

199 We attempted to denoise both long and short PacBio amplicons using DADA2 according to
200 the steps outlined in the supplementary information in Callahan et al. (2019). However, only
201 38 amplicon sequence variants (ASVs) were obtained for the long amplicons, representing 12%
202 of the trimmed reads. We conclude that this poor performance was due to a combination
203 of long read length and low sequencing depth relative to community diversity. The DADA2
204 algorithm requires that the seed sequence of each ASV be represented by at least two error-
205 free reads (Callahan et al., 2016). If sequencing errors are uniformly distributed, then the
206 probability that a given read will be error-free is $(1 - \epsilon)^L$, where ϵ is the sequencing error
207 rate and L is the read length in base pairs. Then the number of reads of a given sequence
208 that would be required to obtain two error-free reads in expectation is $2/(1 - \epsilon)^L$. For
209 the combination of long reads (median $L = 1509$ bp after trimming) and moderate error

210 rate (mean $\epsilon = 0.0073$ based on ccs quality scores) for the long amplicon in this study, the
211 expected number of reads required to achieve two error-free reads is 126,659. Given the
212 high diversity relative to sequencing depth in this study (501 ASVs based on PacBio short
213 amplicons, 108,598 trimmed long amplicon reads), this requirement could not have been met
214 for the long amplicons except by the most abundant sequences. In comparison, the equivalent
215 requirement for the short amplicon ($L = 265$ bp, $\epsilon = 0.0024$) is only 3.8 reads. We therefore
216 developed a new workflow to assemble ASVs from the long amplicons, as follows:

217 Raw reads were divided into shorter regions by matching to covariance models (CM), which
218 are similar to stochastic hidden markov models (HMM), but account for both nucleotide
219 sequence and RNA secondary structure (Eddy & Durbin, 1994). First, the 5.8S rDNA
220 was located in each read by searching for Rfam model RF0002 (Kalvari et al., 2018) using
221 `cmsearch` from Infernal 1.1.2 (Nawrocki & Eddy, 2013), and all bases before the 5.8S were
222 assigned to ITS1. No attempt was made to remove the approximately 12 bp fragment of the
223 SSU from the 5' end of ITS1 in the long amplicons; it was too short to be reliably detected by
224 a CM or the HMMs employed by ITSx (Bengtsson-Palme et al., 2013). A reference alignment
225 including conserved RNA base pairing between and within the 5.8S and relevant portions
226 of LSU was generated from the fungal 28S RNA seed alignment from the Ribosomal Data
227 Project (RDP) release 11.5 (Cole et al., 2014; Glöckner et al., 2017) by truncating after the
228 LR5 primer site and using the reference line to annotate the variable regions *sensu* Michot
229 et al. (1984) and Raué et al. (1988). A CM was generated from the alignment using `cmbuild`
230 from Infernal. The fragment of each read beginning with the 5.8S rDNA was then aligned to
231 the CM using `cmalign` from Infernal. The annotation line in the CM alignment for each read
232 was then used to split the reads into alternating more-conserved and less-conserved regions
233 as shown in Figure S4, where LSU1-4 represent the conserved regions of LSU flanking the
234 variable D1-3 regions (Michot et al., 1984). For short amplicons, only (partial) 5.8S, ITS2,
235 and (partial) LSU1 were extracted. Code to extract the regions, including annotated seed

236 alignments and CMs, is available in the new R package `LSUx`.

237 Each of the extracted regions was independently filtered for length (Supplementary Table S1)
238 and a maximum of three expected errors. Sequences were then dereplicated and denoised
239 into amplicon sequencing variants (ASVs) using DADA2 version 1.12.1 (Callahan et al.,
240 2016; Callahan et al., 2019). The error model for DADA2 denoising was fit using the 5.8S
241 region for long amplicons, and using the entire read for short amplicons. Independent er-
242 ror models were fit for each sequencing run (i.e., long *vs.* short amplicons, different se-
243 quencing technologies). For PacBio libraries, DADA2 was run with complete pooling and
244 a band size of 16. For Ion Torrent libraries, pseudo-pooling and a band size of 32 were
245 used, and the homopolymer gap penalty was set to -1, as recommended by the DADA2 FAQ
246 (<https://benjjneb.github.io/dada2/faq.html>). Chimeras within each region were removed
247 using `removeBimeraDenovoTable` from DADA2.

248 For each ITS2 ASV from the long amplicon data set, the denoised sequences for the other
249 regions corresponding to the same sequencing reads were concatenated to form a set of full-
250 length reads. For reads which were not assigned a denoised sequence for each region, the
251 raw read for the region was used instead. Because ITS2 is the most variable of the amplified
252 regions (Figure S5), reads with identical ITS2 regions are expected to have highly similar
253 sequences in the other regions, unless the amplicon was chimeric. The concatenated ASVs
254 representing each long read were aligned in R using the `DECIPHER` package (Wright, 2015).
255 Outlier sequences, as determined by mean pairwise distance from the rest of the alignment,
256 were removed from each alignment using the `odseq` package (Jehl et al., 2015), using the
257 default threshold of 0.025. The consensus of the remaining aligned sequences was assigned as
258 the full-length ASV sequence. Full-length ASV sequences with more than three ambiguous
259 bases (i.e., no nucleotide >50% at a given position) were removed. The count and sample
260 distribution of reads assigned to each full-length ASV were calculated in order to form a
261 sample \times ASV community matrix. A similar process was used to generate a consensus ITS

262 (ITS1–5.8S–ITS2) and LSU (LSU1–D1–LSU2–D2–LSU3–D3–LSU4) sequence for each ASV.
263 The process of assigning consensus full-length ASVs was carried out using the new `tzara`
264 package for R.

265 Because the Illumina dataset consisted of paired-end reads, regions were not extracted prior
266 to denoising. ASVs were instead generated according to a standard workflow for DADA2.
267 Demultiplexed reads were truncated after the first base with quality score ≤ 10 , and then
268 reads with more than 3 expected errors in either read were discarded. Forward and reverse
269 reads were denoised using DADA2 version 1.12.1 (Callahan et al., 2016) using separate error
270 models and pseudo-pooling, and then forward and reverse reads were merged. The ITS2
271 region was extracted from the ASVs using `LSUx` for comparison to the other technologies.

272 **2.3.2 Taxonomy assignment**

273 Taxonomic annotations of the Ribosomal Data Project’s LSU fungal training set (RDP) ver-
274 sion 11.5 (Cole et al., 2014) and Warcup ITS training set (Deshpande et al., 2016) were
275 mapped to the taxonomic classification system used in the Unite database version 8 (Nilsson
276 et al., 2019). In particular, the classification for fungi was according to Tedersoo, Sánchez-
277 Ramírez, et al. (2018), and for non-fungal eukaryotes was according to the proposed system
278 of Tedersoo (2017a) as described in (Tedersoo, 2017b). Although the latter system is not
279 formally published, it is consistent with the annotations for non-fungal eukaryotes in the
280 Unite database. Additionally, it is a system with both purportedly monophyletic taxa and
281 a uniform set of taxon ranks, which make it more appropriate for sequence-based taxonomic
282 assignment algorithms than more accepted classification systems such as that of the Inter-
283 national Society of Protistologists (Adl et al., 2019), which utilizes hierarchical nameless
284 ranks.

285 Taxonomic assignment was performed to genus level separately on the ITS region using Unite

286 and Warcup and on the LSU region using RDP, respectively, as taxonomic references. For
287 each region/reference combination, taxonomy was assigned using three algorithms: the RDP
288 Naïve Bayesian Classifier (RDPC, Wang et al., 2007) as implemented in DADA2; SINTAX
289 (Edgar, 2016a) as implemented in VSEARCH v2.9.1 (Rognes et al., 2016); and IDTAXA
290 (Murali et al., 2018b). Each full-length ASV was thus given up to nine preliminary taxonomic
291 assignments (three references \times three algorithms). ASVs from the short-amplicon datasets for
292 which no matching long-amplicon ASV could be reconstructed were taxonomically assigned
293 using Unite and Warcup on the full length of the short amplicon.

294 Sequences were assigned as ECM based on taxonomic assignments using the FUNGuild
295 database (Nguyen et al., 2016) via the R package FUNGuildR ([https://github.com/brendanf/](https://github.com/brendanf/FUNGuildR)
296 FUNGuildR). All taxa which included “Ectomycorrhiza” in the guild assignment at any level
297 of confidence were included.

298 **2.3.3 Clustering**

299 For comparison with clustering-based methods, ASVs were clustered into operational taxo-
300 nomic units (OTUs) at 97% similarity using VSEARCH v2.9.1 (Rognes et al., 2016).

301 **2.3.4 Alignment and phylogenetic inference**

302 Full length long amplicon ASVs were aligned using DECIPHER (Wright, 2015) with up to
303 10 iterations of progressive alignment and conserved RNA secondary structure calculation
304 and 10 refinement iterations. This alignment was truncated at a position after the D3 region
305 corresponding to base 907 of the *Saccharomyces cerevisiae* S288C reference sequence for LSU,
306 because several sequences had introns after this position, as also observed in several fungal
307 species by Holst-Jensen et al. (1999).

308 An ML tree was produced using RAxML version 8.2.12 (Stamatakis, 2014) using the

309 GTR+GAMMA model and rapid bootstrapping with the MRE_IGN stopping criterion.
310 The tree was rooted outside the kingdom Fungi by using the most abundant ASV which
311 was confidently assigned to a non-fungal kingdom by all 6 applicable taxonomic assignment
312 methods. Assignments based on Warcup were not used at this step because non-Fungi are
313 not included in the dataset. The kingdom Fungi was identified as the minimal clade con-
314 taining all ASVs which were confidently identified (consensus of at least 6 of 9 assignments)
315 to a fungal phylum. ASVs falling outside this clade were not included in downstream fungal
316 community analysis.

317 Taxonomic assignments of ASVs from the long amplicon dataset were refined using the phy-
318 logenetic tree (Figure S6). A taxon at a particular rank was assigned to a node and all its
319 descendants if that taxon was consistent with the reference-based taxonomic assignments for
320 each of the descendants. A taxon assignment was considered to be consistent if at least one
321 algorithm assigned that taxon at greater than 50% confidence, or if no algorithm successfully
322 classified the sequence at greater than 50% confidence. The result of this process is twofold.
323 First, it gives a taxonomic assignment to ASVs which were previously unassigned if they
324 are nested within a clade which is consistently given an assignment. Second, it clarifies the
325 assignment of ASVs where different algorithms had resulted in different assignments, but
326 only one of these is consistent with the assignments of other ASVs in the same clade. This
327 refinement algorithm is referred to as “PHYLOTAX”.

328 ASVs from the short amplicon datasets were refined using only the final strict consensus step,
329 i.e., an assignment at a given rank was accepted if there was no conflict between the different
330 assignment algorithms at greater than 50% confidence. This refinement method is referred to
331 as “Consensus”. Additionally, a hybrid method, was applied to the short amplicon datasets,
332 in which assignments from PHYLOTAX were used for ASVs which could be linked by an
333 identical ITS2 region to a long amplicon, and assignments from Consensus were used for the
334 remaining ASVs.

335 **2.4 Community comparison**

336 The fungal communities recovered by the three sequencing strategies that were successfully
337 demultiplexed (Illumina, PacBio Short, PacBio Long) were compared by PERMANOVA. In
338 order to detect bias at larger taxonomic scales, ASVs were clustered according to the as-
339 signed taxonomic class. Only samples where all three strategies yielded at least 100 fungal
340 reads (34 samples), and classes which represented at least 1% of reads in at least one sample
341 (14 classes), were included. PERMANOVA included three terms: an indicator for soil sam-
342 ple, comprising all spatiotemporal effects; amplicon length (long vs. short); and sequencing
343 technology (Illumina MiSeq vs. PacBio RS II). The marginal significance of each term for
344 explaining variation in the Bray-Curtis community dissimilarity matrix was performed using
345 the `adonis2` function in the R package `vegan` (Oksanen et al., 2019), with 9999 permuta-
346 tions. Partial Principal Coordinates Analysis (PPCoA) was applied to the same dissimilarity
347 matrix using the `capscale` function in `vegan` (Oksanen et al., 2019). Spatiotemporal effects
348 were partialled out in order to visualize effects due to sequencing technology and amplicon
349 length.

350 A similar analysis was also applied to only fungi classified as ECM, clustered at the family
351 level.

352 **2.5 Spatiotemporal analysis**

353 Turnover scale is the distance at which two communities can be considered to be independent
354 samples of the local species pool. Knowledge of turnover scale is import when planning studies
355 of local diversity and its environmental correlates. It varies between different ecosystems
356 and taxonomic groups. Turnover scale is often measured by the range at which a Mantel
357 correlogram indicates significant autocorrelation, or by fitting a function to an empirical
358 distance-decay curve of community dissimilarity vs. distance (Legendre & Legendre, 2012).

359 Ecological community dissimilarity matrices were calculated using the ASV/OTU based
360 Bray-Curtis metric (both long and short amplicons) and the phylogenetically based weighted
361 UNIFRAC method (only long amplicons) in `phyloseq` version 1.26.0. Each of these distance
362 matrices was used to calculate a Mantel correlogram for distances of 0–12 m. Separate cor-
363 relograms were drawn for samples taken during the same year, and samples separated in
364 time by one year, in order to assess the degree to which the soil community changes over the
365 course of one year.

366 Additionally, empirical distance-decay curves were generated by plotting mean community
367 dissimilarity as a function of spatial distance, and fit to an exponential model of the form
368 given by Legendre and Legendre (2012) using the `nls` function in R. Points in the empirical
369 distance-decay curve were weighted by the number of comparisons within the distance class
370 and the inverse of the distance for the purposes of model fitting. For datasets where the
371 Mantel correlogram indicated spatial correlation between samples taken in separate years,
372 the model was re-fit with an additional term to represent temporal correlation:

$$D = C_0 + C_1 \left[1 - \exp \left(-3 \left(\frac{d}{a_d} + \frac{t}{a_t} \right) \right) \right]$$

373 where D , d , and t represent the community dissimilarity, spatial distance, and time lag
374 between samples, respectively, and the parameters are C_0 , the community dissimilarity from
375 replicate samples (“nugget”); $C_0 + C_1$, the community dissimilarity at long distances (“sill”);
376 a_d the spatial range at which the community dissimilarity has moved 95% of the way from
377 “nugget” to “sill”; and a_t , the equivalent temporal range. The 95% confidence intervals were
378 calculated for the spatial and temporal range parameters by profiling using the `MASS` package
379 in R.

3 Results

DNA concentrations after extraction and PCR, as well as sequencing reads for PacBio and Illumina, are shown per sample in Figure S7. Samples from Ang in 2015 yielded low quantities of DNA, poor PCR performance, and ultimately very few sequencing reads, especially in the long amplicon library, where only one sample produced more than 100 reads. Consequently, Ang samples were excluded from spatial analysis, although they were retained for denoising, phylogenetic reconstruction, and taxonomic assignment.

The number of sequencing reads and ASVs at each stage in the bioinformatics pipeline are shown in Table S2. Sequencing with PacBio RS II yielded more than twice as many raw reads for long amplicons as for short amplicons, with approximately 125 thousand and 50 thousand reads, respectively. Ion Torrent Ion S5 and Illumina MiSeq yielded substantially more reads, with 20.7 million and 10.8 million, respectively. Demultiplexing, primer trimming, and quality filtering reduced these totals by 63% for PacBio long reads, but only by 17% for PacBio short reads, resulting in a similar number of filtered reads for the two strategies. Losses in demultiplexing, trimming, and quality filtering were intermediate for Ion Torrent and Illumina, with 41% and 28% loss, respectively. In contrast, extraction of only the ITS2 region before quality filtering resulted in the loss of 27% of trimmed long amplicon PacBio reads, 19% of trimmed short amplicon PacBio reads, and 34% of trimmed Ion Torrent reads. This represented greater loss of PacBio short reads, but less loss of PacBio long reads and Ion Torrent reads.

Almost all of the short amplicons from all three technologies were between 240 and 375 bp long (Figure S8a). Although the length profile of the three sequencing runs were similar, Illumina MiSeq had the largest fraction of reads near the top of the range, followed by Ion Torrent Ion S5 and PacBio RS II (Figure S8b). The difference in length distributions was statistically significant due to the large sample size (Kruskal-Wallis statistic = 8.5976571×10^4 , $p <$

405 2.2×10^{-16}), but the difference between means was fairly small, with mean amplicon lengths
406 of 274, 281, and 286 bp for PacBio, Ion Torrent, and Illumina, respectively. In contrast, the
407 length of the long amplicon reads varied widely, from 696 to 1638 bp, with a mean of 1432
408 bp.

409 The length distribution of the different regions extracted from the long amplicon are shown
410 in Figure S9. ITS1 showed the greatest length variability (mean \pm standard deviation: 193
411 \pm 55 bp), followed by ITS2 (184 \pm 41 bp) and the variable regions in LSU (D2: 227 \pm 36 bp;
412 D3: 108 \pm 10 bp; D1: 159 \pm 5 bp). Approximately 2% of reads included an intron of 40–60
413 bp in the LSU4 region, not visible in Figure S9 due to rarity. Except for these sequences,
414 all conserved regions of LSU, as well as 5.8S, displayed very little size variation, as expected,
415 with standard deviations $<$ 2 bp.

416 *Agaricus bisporus*, the positive control, was represented by a single ASV in the positive control
417 samples for both long- and short-amplicon PacBio datasets, and in the Ion Torrent dataset.
418 *A. bisporus* was represented by two ASVs in the Illumina dataset, which differed at one base
419 pair (99.5% similarity in ITS2). The abundance of the second ASV was 1.1% and 1.0% that
420 of the primary *A. bisporus* ASV in the two Illumina positive controls. The consistency of this
421 ratio across replicate positive controls suggests that it represents true inter-copy variation
422 within the specimen, rather than sequencing or PCR error. Despite higher total sequencing
423 depth, this ASV was not identified from the Ion Torrent dataset.

424 *A. bisporus* sequences represented 0.11%, 0.08%, 0.10%, and 0.09% of non-control reads,
425 in the PacBio long, PacBio short, Illumina, and Ion Torrent datasets, respectively, giving
426 similar estimates for the rate of tag-switching for all technologies. These reads were excluded
427 from community analyses.

3.1 Reproducibility of sequence capture using different technologies

The majority of abundant ASVs and OTUs were captured by all sequencing strategies used (Figure 1). ASVs shared between all datasets represented 56–79% of the reads for the long and short PacBio datasets, Illumina dataset, and Ion Torrent dataset, respectively. These fractions increased to 73–88% when differences at the intra-species scale were removed by clustering the ASVs into OTUs. In particular, 99%, 92%, and 89% of reads in the PacBio, Illumina, and Ion Torrent short-amplicon datasets belonged to OTUs shared between all three datasets. In contrast, 21% of reads in the long PacBio dataset belonged to ASVs which were unique to that dataset, and the fraction only reduced to 20% after OTU clustering. Complete tabulations of the number of ASVs and OTUs shared between the different sequencing strategies are shown in Supplementary Tables S3 and S4, respectively.

Figure 2 shows the correspondence between the read count for different ASVs (2a) and OTUs(2b) in the different technologies, where shared ASVs/OTUs are plotted as circles, and unshared OTUs are plotted as lines along the axes. In all cases, the read counts for shared ASVs and OTUs were correlated, with a minimum R^2 value of 0.46. Correlations between read counts for the three technologies using the short amplicon library were increased by OTU clustering (0.68 to 0.75, 0.49 to 0.78, and 0.73 to 0.87, for PacBio vs. Illumina, PacBio vs. Ion Torrent, and Illumina vs. Ion Torrent, respectively), but not between the long amplicon library and short amplicon library (0.65 to 0.61, 0.59 to 0.58, and 0.46 to 0.49, for PacBio long amplicon reads vs. PacBio, Illumina, and Ion Torrent short reads, respectively).

449 3.2 Taxonomic assignment

450 For all sequencing datasets and taxonomic assignment protocols, a higher proportion of reads
451 was assigned than of ASVs, indicating that common ASVs were more likely to be identified
452 than rare ASVs (Figure 3). A greater fraction of ITS reads and ASVs were assigned using
453 the Unite database than the Warcup database across sequencing technologies, amplicons,
454 algorithms, and taxonomic ranks. At most taxonomic ranks, the RDPC algorithm assigned
455 the greatest fraction of reads and ASVs, followed by SINTAX, and then IDTAXA.

456 Taxonomic composition of the sequenced soil fungal community at the class level is summarized
457 in Figure 4 and as a heat tree (Foster et al., 2017) in Figure S10. The ML tree for fungal
458 ASVs, along with taxonomic assignments, is shown in Supplementary File 3. According to the
459 PHYLOTAX assignments, Fungi represented 76% of the ASVs and 90% of the reads in the
460 long amplicon library, compared to 89.7%–94.7% of the ASVs and 98.4%–98.9% of the reads
461 in the short amplicon library. Measured fungal community composition at the class level
462 varied significantly between amplicons (PERMANOVA with 9999 permutations, $p < 0.0001$,
463 $R^2 = 0.046$), but only marginally between sequencing technologies ($p = 0.0613$, $R^2 = 0.001$).
464 The majority of variation was spatiotemporal (i.e., between samples; $p < 0.0001$, $R^2 = 0.90$),
465 but once this variation was removed, the remaining effect consisted of a clear bias against
466 Sordariomycetes in the long amplicon dataset (Figures 4 and S12).

467 Fungi categorized as ECM made up 8.2% of ASVs and 39.0% of reads in the long amplicon
468 library, and 6.2%–13.3% of the ASVs and 36.1%–47.0% of the reads in the short amplicon
469 library (Figure S11). Although amplicon length had a significant effect on ECM community
470 composition at the family level, the explained variation was very low (PERMANOVA with
471 9999 permutations, $p = 0.0009$, $R^2 = 0.002$), and the majority of variation was again
472 spatiotemporal ($p < 0.0001$, $R^2 = 0.98$). Variation between sequencing technologies was not
473 significant ($p = 0.47$, $R^2 = 0.0004$).

474 3.3 Spatial analysis

475 Results of spatial analysis based on the Bray-Curtis dissimilarity were qualitatively similar
476 between the two amplicon libraries and between PacBio and Illumina sequencing, with sig-
477 nificant autocorrelation at $p < 0.05$ for ranges of up to 2–3 m for the total fungal community,
478 and 1–2 m for the ECM fungal community (Figure S13). In both cases, the greatest corre-
479 lation magnitudes were found with Illumina, followed by long amplicon PacBio. The least
480 spatial structure was detected with PacBio short amplicon sequencing.

481 The Bray-Curtis metric showed significant ($p < 0.05$) positive correlation when resampling
482 at the same locations one year later (i.e., spatial distance of 0 m, time lag of 1 year), for both
483 the total fungal and ECM fungal communities in the long amplicon library. For the short
484 amplicon library, although the general profile of the correlograms was similar, correlation at
485 0 m and 1 year was not significant, but there was a negative correlation at time lag of 1 year
486 and a distance of 1 m for both sequencing technologies. This puzzling negative correlation was
487 significant in all correlograms based on short amplicon sequencing irrespective of technology.

488 In contrast to the Bray-Curtis distance, the weighted UNIFRAC distance showed very little
489 spatial structure, with only the total fungal community in the 1 m distance class showing
490 a significant correlation at $p < 0.05$. No temporal correlation was found for the weighted
491 UNIFRAC distance.

492 The best fit spatial ranges based on distance-decay curves vary between the different datasets
493 by a factor of about 3, but there is overlap of the 95% confidence intervals for all of the Bray-
494 Curtis spatial ranged in both the total fungal and ECM fungal communities, across amplicon
495 libraries and sequencing technologies (Figure 5, Table S5). Although a distance-decay model
496 was fit for the weighted UNIFRAC distance applied to the total fungal community, the result
497 was very poorly constrained, and a range of 0 m, indicating no spatial structure, was included
498 in the 95% confidence interval.

499 **4 Discussion**

500 **4.1 Reconstruction of long amplicons from denoised subregions**

501 ASV recovery for long amplicons using DADA2 was dramatically improved (12% to 75% of
502 reads) by denoising homologous subregions independently using the `LSUx` and `tzara` pack-
503 ages. Although newer sequencing platforms from PacBio (Sequel and Sequel II) feature
504 increased sequencing depth and lower error rate compared to the RS II, long sequences
505 inherently require much more sampling depth to identify ASVs. Thus, `tzara` should in-
506 crease ASV recovery from these platforms as well. It may also be adaptable to Oxford
507 Nanopore sequencing, which has hitherto posed difficulties for application to complex com-
508 munity metabarcoding (Loit et al., 2019).

509 **4.2 Comparison of sequencing strategies**

510 The three sequencing technologies gave similar results for the short amplicon library, the
511 major difference being in sequencing depth. Although a greater fraction of PacBio raw reads
512 were ultimately mapped to ASVs (76%) compared to Illumina (63%) or Ion Torrent (65%),
513 the latter two technologies provided much greater sequencing depth for a similar cost, allowing
514 a greater diversity of rare ASVs to be recovered.

515 DADA2 denoising may perform differently on different technologies (or perhaps sequencing
516 runs), indicated by the fact that clustering ASVs at 97% led to substantially higher corre-
517 spondence between both the set of sequences recovered from the same library by different
518 technologies (Figure 1) and the read counts for each sequence (Figure 2). The large num-
519 ber of ASVs unique to Ion Torrent, while only the Illumina dataset recovered an apparent
520 intragenomic variant in the positive control sample, suggests that DADA2 may not con-
521 trol sequencing error as effectively in Ion Torrent sequences as in Illumina, for which it was

522 developed (Callahan et al., 2016).

523 Although the longer read length capabilities of PacBio would allow recovery of longer ITS2
524 sequences than the other two technologies, PacBio did not recover any ITS2 fragments longer
525 than those recovered by Illumina and Ion Torrent. Notably, neither long nor short amplicon
526 sequencing recovered any sequences identifiable to *Cantharellus*, an ECM genus which is
527 commonly observed at the study sites as fruitbodies (personal observation), but which is
528 also known to have accelerated evolution in the rDNA (Moncalvo et al., 2006) and longer
529 ITS regions than other fungi (Feibelman et al., 1994), making it an especially difficult target
530 for metabarcoding. Contrary to expectations, Illumina showed a slightly higher fraction of
531 longer ITS2 sequences than Ion Torrent, which in turn showed slightly longer sequences than
532 PacBio (Figures S8 and S14).

533 Of long amplicon reads, 21% belonged to ASVs which occurred only in the long amplicon
534 dataset, and clustering at 97% similarity only reduced this fraction to 20%. Additionally,
535 ITS2 sequences extracted from the long amplicon dataset included some sequences that were
536 much shorter than those recovered from the short amplicon datasets (Figure S14). Taxonomic
537 assignments revealed that the majority of these non-shared sequences fall outside kingdom
538 Fungi (Figure S15), and that in particular the short ITS2 sequences are mostly Alveolates
539 (Figure S16). Within Fungi, the short amplicon datasets recovered more Sordariomycetes
540 (Figures 4, S12, and S15). Additionally, several smaller groups showed increased detection
541 in either the long or short datasets, such as Tulasnellaceae and Pyronemataceae in the long
542 amplicon dataset, and *Myerozyma* in the short amplicon datasets (Figures S15 and S17).
543 These differences may be due to primer mismatches in these taxa.

544 4.3 Taxonomic identification

545 The RDP fungal training set and Unite performed comparably at taxonomic placement of
546 long amplicon sequences. The Warcup database placed notably fewer sequences at all tax-
547 onomic levels for all datasets, probably in part due to the fact that only fungal sequences
548 are included. However, even with this considered, IDTAXA performed very poorly with the
549 Warcup database, placing <25% of ASVs to kingdom in all datasets. IDTAXA placed fewer
550 sequences than RDPC or SINTAX even with the other databases, but this is expected given
551 its more conservative assignment of confidence scores (Murali et al., 2018a).

552 Gdanetz et al. (2017) showed that a majority-rule consensus of three assignment algorithms
553 can improve the fraction of sequences assigned as well as decrease the false assignment rate.
554 Strict consensus rejects assignments whenever there is conflict between methods and should
555 therefore provide more conservative taxonomic assignments than majority-rule consensus.
556 Here, we found that strict consensus also usually increases the number of assigned sequences
557 relative to any single method, except at family and genus level identifications. This sug-
558 gests that different assignment algorithms and databases bring mostly complementary, non-
559 contradictory information at higher taxonomic levels. However, contradictory assignments
560 between different methods is more common at lower taxonomic levels, which can be prob-
561 lematic because accurate assignment at the family or genus level is generally required for
562 ecological guild assignment using FUNGuild.

563 For ASVs where a long amplicon sequence is available, PHYLOTAX uses phylogenetic re-
564 lationships to resolve these disagreements in a principled manner. For instance, 56% and
565 83% of Illumina reads were assigned to genus and family, respectively, by the strict consen-
566 sus of methods, but PHYLOTAX increased this fraction to 77% and 94%. This led to a
567 corresponding increase in the fraction of reads assigned to a functional guild (Figure S11).

568 4.4 Turnover rate

569 Weighted UNIFRAC did not reliably detect spatial structure within this relatively ecologi-
570 cally homogeneous community. Although the Mantel test did show a small but significant
571 positive autocorrelation in the fungal community at the smallest size category (1 m; Fig-
572 ure S13), the distance-decay plot in Figure 5 does not show any clear relationship. The
573 functional fit showed poor convergence, with a 95% confidence interval for spatial range of
574 0–5700 m, indicating little evidence of spatial structure. This is probably due to the ma-
575 jority of weighted branch length in the community being between the Pezizomycotina and
576 Agaricomycetes (Figure S10), which are both well represented in the majority of samples.
577 UNIFRAC would be more suited at larger spatial scales and/or larger ecological gradients.

578 Mantel correlograms based on the Bray-Curtis dissimilarity (Figure S13) revealed spatial
579 autocorrelation in the soil fungal community at distance classes ≤ 3 m for both Illumina and
580 PacBio using long and short amplicons, and in the ECM fungal community at distance classes
581 ≤ 2 m for Illumina and PacBio long amplicons, and ≤ 1 m for the PacBio short amplicons.
582 These results are similar to autocorrelation ranges found in previous work based on ECM
583 root tips in temperate forests (Lilleskov et al., 2004; Pickles et al., 2012). Lilleskov et al.
584 (2004) found autocorrelation only at ranges < 2.6 m at most sites using Sanger sequencing.
585 Similarly, Pickles et al. (2012) found autocorrelation at distances < 3.4 m based on T-RFLP
586 analysis. However, previous work in Miombo woodland, a similar ecosystem to the Soudanian
587 woodland in this study, found autocorrelation at ranges < 10 m using Sanger sequencing of
588 ECM root tips (Tedersoo et al., 2011), which was their smallest distance class.

589 Distance-decay plots (Figure 5, Table S5) gave substantially longer autocorrelation distances.
590 There was little variation in the results between the Illumina and long-amplicon PacBio
591 datasets for both the total fungal community and the ECM community, with best fit esti-
592 mates ranging from 13–19 m. The 95% confidence interval was substantially wider than this

593 variation, generally covering a range of 6–44 m. All of these values are smaller than the
594 65 m reported by Bahram et al. (2013), also based on distance-decay curves from an ECM
595 woodland habitat in Benin.

596 The PacBio short amplicon dataset shows a longer spatial range, of 31 m for the total
597 fungal community and 42–42 m for the ECM community, in both cases with wide confidence
598 intervals spanning 15–203 m. It is possible that the weaker fit for this dataset, which also
599 showed weaker autocorrelation in the Mantel correlogram, is due to low sequencing depth.

600 The Bray-Curtis Mantel correlogram for both the total fungal and ECM communities from
601 the long amplicon dataset show a significant positive correlation at 0 m and 1 year. The
602 spatiotemporal distance-decay fit estimated the temporal turnover range as 3.1 years for
603 the total fungal community and 4.0 years for the ECM community, but with overlapping
604 confidence intervals. Both datasets from the short amplicon library showed a puzzling pattern
605 with no autocorrelation at 0 m and 1 year, but a weak negative correlation at 1 m and 1 year.
606 The general shape of the correlograms were similar for long and short amplicon datasets. We
607 hypothesize that two different processes may be at work with differing spatiotemporal scales,
608 whose superposition result in this pattern.

609 **4.5 Conclusion**

610 The choice of amplicon and sequencing technology did not seem to affect the results of the
611 spatial analysis, provided sufficient sequencing depth. However, the addition of long amplicon
612 reads did allow the construction of a phylogenetic tree from the metabarcoding reads, which
613 allowed refinement of taxonomic assignments. DADA2 ASV yield was initially poor for
614 long reads, but this was improved by developing a workflow for extraction of subregions,
615 separate denoising, and then reconstruction of full-length unique sequences. Together these
616 approaches provide a hybrid approach using long-read sequencing to acquire long amplicon

617 sequences for the local species pool, and cost-effective short-read sequencing to provide high
618 sampling depth and sample number.

619 **Acknowledgements**

620 This project was funded by the Swedish research council FORMAS grant number 2014-01109.

621 Laboratory work including PCR and library pooling was performed by Dr. Ylva Strid.

622 The authors would like to acknowledge support of the National Genomics Infrastructure
623 (NGI) / Uppsala Genome Center and UPPMAX for providing assistance in massive parallel
624 sequencing and computational infrastructure. Work performed at NGI / Uppsala Genome
625 Center has been funded by RFI / VR and and Science for Life Laboratory, Sweden.

626 Sequencing was performed by the SNP&SEQ Technology Platform in Uppsala. The facility is
627 part of the National Genomics Infrastructure (NGI) Sweden and Science for Life Laboratory.
628 The SNP&SEQ Platform is also supported by the Swedish Research Council and the Knut
629 and Alice Wallenberg Foundation.

630 **References**

- 631 Adl, S. M., Bass, D., Lane, C. E., Lukeš, J., Schoch, C. L., Smirnov, A., Agatha, S., Berney,
632 C., Brown, M. W., Burki, F., Cárdenas, P., Čepička, I., Chistyakova, L., Campo, J. del,
633 Dunthorn, M., Edvardsen, B., Eglit, Y., Guillou, L., Hampl, V., ... Zhang, Q. (2019).
634 Revisions to the Classification, Nomenclature, and Diversity of Eukaryotes. *Journal*
635 *of Eukaryotic Microbiology*, 66(1), 4–119. <https://doi.org/10.1111/jeu.12691>
- 636 Ainsworth, G. C. (2008). *Ainsworth & Bisby's dictionary of the fungi*. Cabi.
- 637 Altschul, S. F., Gish, W., Miller, W., Myers, E. W., & Lipman, D. J. (1990). Basic local
638 alignment search tool. *Journal of Molecular Biology*, 215(3)pmid 2231712, 403–410.
639 [https://doi.org/10.1016/S0022-2836\(05\)80360-2](https://doi.org/10.1016/S0022-2836(05)80360-2)
- 640 Amir, A., McDonald, D., Navas-Molina, J. A., Kopylova, E., Morton, J. T., Xu, Z. Z., Kight-
641 ley, E. P., Thompson, L. R., Hyde, E. R., Gonzalez, A., & Knight, R. (2017). De-
642 blur Rapidly Resolves Single-Nucleotide Community Sequence Patterns. *mSystems*,
643 2(2)pmid 28289731, e00191–16. <https://doi.org/10.1128/mSystems.00191-16>

- 644 Bahram, M., Koljalg, U., Courty, P.-E., Diedhiou, A. G., Kjølner, R., Polme, S., Ryberg, M.,
645 Veldre, V., & Tedersoo, L. (2013). The distance decay of similarity in communities of
646 ectomycorrhizal fungi in different ecosystems and scales. *Journal of Ecology*, *101*(5),
647 1335–1344.
- 648 Bengtsson-Palme, J., Ryberg, M., Hartmann, M., Branco, S., Wang, Z., Godhe, A., Wit,
649 P. D., Sánchez-García, M., Ebersberger, I., Sousa, F. de, Amend, A., Jumpponen,
650 A., Unterseher, M., Kristiansson, E., Abarenkov, K., Bertrand, Y. J. K., Sanli, K.,
651 Eriksson, K. M., Vik, U., ... Nilsson, R. H. (2013). Improved software detection and
652 extraction of ITS1 and ITS2 from ribosomal ITS sequences of fungi and other eukary-
653 otes for analysis of environmental sequencing data. *Methods in Ecology and Evolution*,
654 *4*(10), 914–919. <https://doi.org/10.1111/2041-210X.12073>
- 655 Berger, S. A., Krompass, D., & Stamatakis, A. (2011). Performance, Accuracy, and Web
656 Server for Evolutionary Placement of Short Sequence Reads under Maximum Likeli-
657 hood. *Systematic Biology*, *60*(3), 291–302. <https://doi.org/10.1093/sysbio/syr010>
- 658 Brundrett, M. C. (2017). Global Diversity and Importance of Mycorrhizal and Nonmycor-
659 rhizal Plants. In L. Tedersoo (Ed.), *Biogeography of Mycorrhizal Symbiosis* (pp. 533–
660 556). Cham, Springer International Publishing. https://doi.org/10.1007/978-3-319-56363-3_21
- 662 Callahan, B. J., McMurdie, P. J., & Holmes, S. P. (2017). Exact sequence variants should
663 replace operational taxonomic units in marker-gene data analysis. *The ISME Journal*,
664 *11*(12), 2639–2643. <https://doi.org/10.1038/ismej.2017.119>
- 665 Callahan, B. J., McMurdie, P. J., Rosen, M. J., Han, A. W., Johnson, A. J. A., & Holmes,
666 S. P. (2016). DADA2: High-resolution sample inference from Illumina amplicon data.
667 *Nature Methods*, *13*(7), 581–583. <https://doi.org/10.1038/nmeth.3869>
- 668 Callahan, B. J., Wong, J., Heiner, C., Oh, S., Theriot, C. M., Gulati, A. S., McGill, S. K., &
669 Dougherty, M. K. (2019). High-throughput amplicon sequencing of the full-length 16S
670 rRNA gene with single-nucleotide resolution. *Nucleic Acids Research*, *47*(18), e103–
671 e103. <https://doi.org/10.1093/nar/gkz569>
- 672 Cole, J. R., Wang, Q., Fish, J. A., Chai, B., McGarrell, D. M., Sun, Y., Brown, C. T.,
673 Porras-Alfaro, A., Kuske, C. R., & Tiedje, J. M. (2014). Ribosomal Database Project:
674 Data and tools for high throughput rRNA analysis. *Nucleic Acids Research*, *42*(D1),
675 D633–D642. <https://doi.org/10.1093/nar/gkt1244>
- 676 Deshpande, V., Wang, Q., Greenfield, P., Charleston, M., Porras-Alfaro, A., Kuske, C. R.,
677 Cole, J. R., Midgley, D. J., & Tran-Dinh, N. (2016). Fungal identification using a
678 Bayesian classifier and the Warcup training set of internal transcribed spacer se-
679 quences. *Mycologia*, *108*(1), 1–5. <https://doi.org/10.3852/14-293>
- 680 Eddy, S. R., & Durbin, R. (1994). RNA sequence analysis using covariance models. *Nucleic*
681 *Acids Research*, *22*(11), 2079–2088. <https://doi.org/10.1093/nar/22.11.2079>
- 682 Edgar, R. C. (2016a). SINTAX: A simple non-Bayesian taxonomy classifier for 16S and ITS
683 sequences. *bioRxiv*, 074161. <https://doi.org/10.1101/074161>
- 684 Edgar, R. C. (2016b). UNOISE2: Improved error-correction for Illumina 16S and ITS ampli-
685 con sequencing. *bioRxiv*, 081257. <https://doi.org/10.1101/081257>

- 686 Feibelman, T., Bayman, P., & Cibula, W. G. (1994). Length variation in the internal tran-
687 scribed spacer of ribosomal DNA in chanterelles. *Mycological Research*, 98(6), 614–
688 618. [https://doi.org/10.1016/s0953-7562\(09\)80407-3](https://doi.org/10.1016/s0953-7562(09)80407-3)
- 689 Foster, Z. S. L., Sharpton, T. J., & Grünwald, N. J. (2017). Metacoder: An R package
690 for visualization and manipulation of community taxonomic diversity data. *PLOS*
691 *Computational Biology*, 13(2), e1005404. [https://doi.org/10.1371/journal.pcbi.](https://doi.org/10.1371/journal.pcbi.1005404)
692 1005404
- 693 [Dataset] Furneaux, B., Bahram, M., Rosling, A., Yorou, N. S., & Ryberg, M. (2020). *Data*
694 *for "Long- and short-read metabarcoding reveal similar spatio-temporal structures in*
695 *fungal communities"*. Dryad. <https://doi.org/XXXX>
- 696 Gdanetz, K., Benucci, G. M. N., Vande Pol, N., & Bonito, G. (2017). CONSTAX: A tool for
697 improved taxonomic resolution of environmental fungal ITS sequences. *BMC Bioin-*
698 *formatics*, 18(1), 538. <https://doi.org/10.1186/s12859-017-1952-x>
- 699 Glöckner, F. O., Yilmaz, P., Quast, C., Gerken, J., Beccati, A., Ciuprina, A., Bruns, G., Yarza,
700 P., Peplies, J., Westram, R., & Ludwig, W. (2017). 25 years of serving the community
701 with ribosomal RNA gene reference databases and tools. *Journal of Biotechnology*,
702 261, 169–176. <https://doi.org/10.1016/j.jbiotec.2017.06.1198>
- 703 Holst-Jensen, A., Vaage, M., Schumacher, T., & Johansen, S. (1999). Structural characteris-
704 tics and possible horizontal transfer of group I introns between closely related plant
705 pathogenic fungi. *Molecular Biology and Evolution*, 16(1), 114–126. [https://doi.org/](https://doi.org/10.1093/oxfordjournals.molbev.a026031)
706 10.1093/oxfordjournals.molbev.a026031
- 707 Horton, T. R., & Bruns, T. D. (2001). The molecular revolution in ectomycorrhizal ecology:
708 Peeking into the black-box. *Molecular Ecology*, 10(8), 1855–1871. [https://doi.org/10.](https://doi.org/10.1046/j.0962-1083.2001.01333.x)
709 1046/j.0962-1083.2001.01333.x
- 710 Ihrmark, K., Bödeker, I. T. M., Cruz-Martinez, K., Friberg, H., Kubartova, A., Schenck,
711 J., Strid, Y., Stenlid, J., Brandström-Durling, M., Clemmensen, K. E., & Lindahl,
712 B. D. (2012). New primers to amplify the fungal ITS2 region – evaluation by 454-
713 sequencing of artificial and natural communities. *FEMS Microbiology Ecology*, 82(3),
714 666–677. <https://doi.org/10.1111/j.1574-6941.2012.01437.x>
- 715 Jehl, P., Sievers, F., & Higgins, D. G. (2015). OD-seq: Outlier detection in multiple sequence
716 alignments. *BMC Bioinformatics*, 16(1), 269. [https://doi.org/10.1186/s12859-015-](https://doi.org/10.1186/s12859-015-0702-1)
717 0702-1
- 718 Kalvari, I., Nawrocki, E. P., Argasinska, J., Quinones-Olvera, N., Finn, R. D., Bateman, A.,
719 & Petrov, A. I. (2018). Non-Coding RNA Analysis Using the Rfam Database. *Current*
720 *Protocols in Bioinformatics*, 62(1), e51. <https://doi.org/10.1002/cpbi.51>
- 721 Kennedy, P. G., Cline, L. C., & Song, Z. (2018). Probing promise versus performance in
722 longer read fungal metabarcoding. *New Phytologist*, 217(3), 973–976.
- 723 Legendre, P., & Legendre, L. F. J. (2012, July 21). *Numerical Ecology*. Elsevier.
- 724 Lilleskov, E. A., Bruns, T. D., Horton, T. R., Taylor, D. L., & Grogan, P. (2004). Detection
725 of forest stand-level spatial structure in ectomycorrhizal fungal communities. *FEMS*
726 *Microbiology Ecology*, 49(2), 319–332. <https://doi.org/10.1016/j.femsec.2004.04.004>
- 727 Lindahl, B. D., Nilsson, R. H., Tedersoo, L., Abarenkov, K., Carlsen, T., Kjølner, R., Kõljalg,
728 U., Pennanen, T., Rosendahl, S., Stenlid, J., et al. (2013). Fungal community analysis

729 by high-throughput sequencing of amplified markers—a user’s guide. *New Phytologist*,
730 199(1), 288–299.

731 Loit, K., Adamson, K., Bahram, M., Puusepp, R., Anslan, S., Kiiker, R., Drenkhan, R., &
732 Tedersoo, L. (2019). Relative Performance of MinION (Oxford Nanopore Technolo-
733 gies) versus Sequel (Pacific Biosciences) Third-Generation Sequencing Instruments in
734 Identification of Agricultural and Forest Fungal Pathogens. *Applied and Environmen-
735 tal Microbiology*, 85(21)pmid 31444199. <https://doi.org/10.1128/AEM.01368-19>

736 Martin, M. (2011). Cutadapt removes adapter sequences from high-throughput sequencing
737 reads. *EMBnet.journal*, 17(1), 10–12. <https://doi.org/10.14806/ej.17.1.200>

738 Matsen, F. A., Kodner, R. B., & Armbrust, E. V. (2010). Pplacer: Linear time maximum-
739 likelihood and Bayesian phylogenetic placement of sequences onto a fixed reference
740 tree. *BMC Bioinformatics*, 11(1), 538. <https://doi.org/10.1186/1471-2105-11-538>

741 Michot, B., Hassouna, N., & Bachellerie, J.-P. (1984). Secondary structure of mouse 28S
742 rRNA and general model for the folding of the large rRNA in eukaryotes. *Nucleic
743 Acids Research*, 12(10), 4259–4279. <https://doi.org/10.1093/nar/12.10.4259>

744 Moncalvo, J.-M., Nilsson, R. H., Koster, B., Dunham, S. M., Bernauer, T., Matheny, P. B.,
745 Porter, T. M., Margaritescu, S., Weiß, M., Garnica, S., Danell, E., Langer, G., Langer,
746 E., Larsson, E., Larsson, K.-H., & Vilgalys, R. (2006). The cantharelloid clade: Deal-
747 ing with incongruent gene trees and phylogenetic reconstruction methods. *Mycologia*,
748 98(6), 937–948. <https://doi.org/10.1080/15572536.2006.11832623>

749 Murali, A., Bhargava, A., & Wright, E. S. (2018a). IDTAXA: A novel approach for accurate
750 taxonomic classification of microbiome sequences. *Microbiome*, 6(1), 140. [https://doi.
751 org/10.1186/s40168-018-0521-5](https://doi.org/10.1186/s40168-018-0521-5)

752 Murali, A., Bhargava, A., & Wright, E. S. (2018b). IDTAXA: A novel approach for accurate
753 taxonomic classification of microbiome sequences. *Microbiome*, 6(1), 140. [https://doi.
754 org/10.1186/s40168-018-0521-5](https://doi.org/10.1186/s40168-018-0521-5)

755 Nawrocki, E. P., & Eddy, S. R. (2013). Infernal 1.1: 100-fold faster RNA homology searches.
756 *Bioinformatics*, 29(22), 2933–2935. <https://doi.org/10.1093/bioinformatics/btt509>

757 Nguyen, N. H., Song, Z., Bates, S. T., Branco, S., Tedersoo, L., Menke, J., Schilling, J. S.,
758 & Kennedy, P. G. (2016). FUNGuild: An open annotation tool for parsing fungal
759 community datasets by ecological guild. *Fungal Ecology*, 20, 241–248.

760 Nilsson, R. H., Larsson, K.-H., Taylor, A. F. S., Bengtsson-Palme, J., Jeppesen, T. S., Schigel,
761 D., Kennedy, P., Picard, K., Glöckner, F. O., Tedersoo, L., Saar, I., Kõljalg, U., &
762 Abarenkov, K. (2019). The UNITE database for molecular identification of fungi:
763 Handling dark taxa and parallel taxonomic classifications. *Nucleic Acids Research*,
764 47(D1), D259–D264. <https://doi.org/10.1093/nar/gky1022>

765 Oksanen, J., Blanchet, F. G., Friendly, M., Kindt, R., Legendre, P., McGlinn, D., Minchin,
766 P. R., O’Hara, R. B., Simpson, G. L., Solymos, P., Stevens, M. H. H., Szoecs, E., &
767 Wagner, H. (2019). *Vegan: Community ecology package* [R package version 2.5-6]. R
768 package version 2.5-6. <https://CRAN.R-project.org/package=vegan>

769 Pacific Biosciences. (2019, February 22). *Consensus library and applications. Contribute to
770 PacificBiosciences/unanimity development by creating an account on GitHub*. Re-
771 trieved March 11, 2019, from <https://github.com/PacificBiosciences/unanimity>

- 772 Pickles, B. J., Genney, D. R., Anderson, I. C., & Alexander, I. J. (2012). Spatial analysis of
773 ectomycorrhizal fungi reveals that root tip communities are structured by competitive
774 interactions. *Molecular Ecology*, *21*(20), 5110–5123. <https://doi.org/10.1111/j.1365-294X.2012.05739.x>
775
- 776 Raué, H. A., Klootwijk, J., & Musters, W. (1988). Evolutionary conservation of structure
777 and function of high molecular weight ribosomal RNA. *Progress in Biophysics and*
778 *Molecular Biology*, *51*(2), 77–129. [https://doi.org/10.1016/0079-6107\(88\)90011-9](https://doi.org/10.1016/0079-6107(88)90011-9)
- 779 Rinaldi, A., Comandini, O., & Kuyper, T. W. (2008). Ectomycorrhizal fungal diversity:
780 Separating the wheat from the chaff. *Fungal Diversity*, *33*, 1–45.
- 781 Rognes, T., Flouri, T., Nichols, B., Quince, C., & Mahé, F. (2016). VSEARCH: A versatile
782 open source tool for metagenomics. *PeerJ*, *4*, e2584. <https://doi.org/10.7717/peerj.2584>
783
- 784 Ryberg, M. (2015). Molecular operational taxonomic units as approximations of species in
785 the light of evolutionary models and empirical data from Fungi. *Molecular Ecology*,
786 *24*(23), 5770–5777. <https://doi.org/10.1111/mec.13444>
- 787 Schoch, C. L., Seifert, K. A., Huhndorf, S., Robert, V., Spouge, J. L., Levesque, C. A., Chen,
788 W., & Consortium, F. B. (2012). Nuclear ribosomal internal transcribed spacer (ITS)
789 region as a universal DNA barcode marker for Fungi. *Proceedings of the National*
790 *Academy of Sciences*, *109*(16)pmid 22454494, 6241–6246. <https://doi.org/10.1073/pnas.1117018109>
791
- 792 Smith, S. E., & Read, D. J. (2010). *Mycorrhizal symbiosis*. Academic press.
- 793 Somervuo, P., Koskela, S., Pennanen, J., Henrik Nilsson, R., & Ovaskainen, O. (2016). Unbi-
794 ased probabilistic taxonomic classification for DNA barcoding. *Bioinformatics*, *32*(19),
795 2920–2927. <https://doi.org/10.1093/bioinformatics/btw346>
- 796 Stamatakis, A. (2014). RAxML version 8: A tool for phylogenetic analysis and post-analysis
797 of large phylogenies. *Bioinformatics*, *30*(9), 1312–1313. <https://doi.org/10.1093/bioinformatics/btu033>
798
- 799 Tedersoo, L. (2017a). Proposal for practical multi-kingdom classification of eukaryotes based
800 on monophyly and comparable divergence time criteria. *bioRxiv*, 240929. <https://doi.org/10.1101/240929>
801
- 802 [Dataset] Tedersoo, L. (2017b). *Proposed practical classification of the domain Eukarya based*
803 *on the NCBI system and monophyly and comparable divergence time criteria*. PlutoF.
804 <https://doi.org/10.15156/BIO/587483>
- 805 Tedersoo, L., Anslan, S., Bahram, M., Pölme, S., Riit, T., Liiv, I., Kõljalg, U., Kisand, V.,
806 Nilsson, H., Hildebrand, F., Bork, P., & Abarenkov, K. (2015). Shotgun metagenomes
807 and multiple primer pair-barcode combinations of amplicons reveal biases in metabar-
808 coding analyses of fungi. *MycKeys*, *10*, 1–43. <https://doi.org/10.3897/mycokeys.10.4852>
809
- 810 Tedersoo, L., Bahram, M., Jairus, T., Bechem, E., Chinoya, S., Mpumba, R., Leal, M.,
811 Randrianjohany, E., Razafimandimbison, S., Sadam, A., et al. (2011). Spatial structure
812 and the effects of host and soil environments on communities of ectomycorrhizal fungi
813 in wooded savannas and rain forests of Continental Africa and Madagascar. *Molecular*

814 *Ecology*, 20(14), 3071–3080. Retrieved March 10, 2016, from <http://onlinelibrary.wiley.com/doi/10.1111/j.1365-294X.2011.05145.x/full>

815

816 Tedersoo, L., Sánchez-Ramírez, S., Kõljalg, U., Bahram, M., Döring, M., Schigel, D., May, T., Ryberg, M., & Abarenkov, K. (2018). High-level classification of the Fungi and a tool for evolutionary ecological analyses. *Fungal Diversity*. <https://doi.org/10.1007/s13225-018-0401-0>

817

818

819

820 Tedersoo, L., Tooming-Klunderud, A., & Anslan, S. (2018). PacBio metabarcoding of Fungi and other eukaryotes: Errors, biases and perspectives. *New Phytologist*, 217(3), 1370–1385.

821

822

823 Urbina, H., Scofield, D. G., Cafaro, M., & Rosling, A. (2016). DNA-metabarcoding uncovers the diversity of soil-inhabiting fungi in the tropical island of Puerto Rico. *Mycoscience*, 57(3), 217–227. <https://doi.org/10.1016/j.myc.2016.02.001>

824

825

826 Vesterinen, E. J., Ruokolainen, L., Wahlberg, N., Peña, C., Roslin, T., Laine, V. N., Vasko, V., Sääksjärvi, I. E., Norrdahl, K., & Lilley, T. M. (2016). What you need is what you eat? Prey selection by the bat *Myotis daubentonii*. *Molecular Ecology*, 25(7), 1581–1594. <https://doi.org/10.1111/mec.13564>

827

828

829

830 Vilgalys, R., & Hester, M. (1990). Rapid genetic identification and mapping of enzymatically amplified ribosomal DNA from several *Cryptococcus* species. *Journal of Bacteriology*, 172(8) PMID 2376561, 4238–4246. <https://doi.org/10.1128/jb.172.8.4238-4246.1990>

831

832

833 Wang, Q., Garrity, G. M., Tiedje, J. M., & Cole, J. R. (2007). Naïve Bayesian Classifier for Rapid Assignment of rRNA Sequences into the New Bacterial Taxonomy. *Appl. Environ. Microbiol.*, 73(16) PMID 17586664, 5261–5267. <https://doi.org/10.1128/AEM.00062-07>

834

835

836

837 White, T., Bruns, T., Lee, S., & Taylor, J. (1990). Amplification and direct sequencing of fungal ribosomal RNA genes for phylogenetics. In M. Innis, D. Gelfand, J. Sninsky, & T. White (Eds.), *PCR Protocols: A Guide to Methods and Applications* (pp. 315–322). Academic Press, Inc.

838

839

840

841 Wong, R. G., Wu, J. R., & Gloor, G. B. (2016). Expanding the UniFrac Toolbox. *PLOS ONE*, 11(9), e0161196. <https://doi.org/10.1371/journal.pone.0161196>

842

843 Wright, E. S. (2015). DECIPHER: Harnessing local sequence context to improve protein multiple sequence alignment. *BMC Bioinformatics*, 16(1), 322. <https://doi.org/10.1186/s12859-015-0749-z>

844

845

846 Data Accessibility

- 847 • Sequence data, including raw reads and ASV sequences, will be deposited at the European Nucleotide Archive (ENA) prior to final publication.
- 848
- 849 • Nucleotide alignment and ML tree will be deposited at Dryad prior to final publication

850 (Furneau et al., 2020).

- 851 • R packages `LSUx`, `tzara`, `phylotax`, and `FUNGuildR` are available on Github at
852 <https://github.com/brendanf/LSUx>, <https://github.com/brendanf/tzara>, <https://github.com/brendanf/phylotax>, and <https://github.com/brendanf/FUNGuildR>.
853 These packages are currently being prepared for submission to Bioconductor. If they
854 are not accepted at Bioconductor prior to final publication, they will be archived at
855 Dryad.
856
- 857 • FASTA-format files for the RDP, Warcup, and Unite reference databases with unified
858 classifications, as well as scripts used to generate them, are available at <https://github.com/brendanf/reannotate>. The versions used in this paper will be archived at Dryad
859 prior to publication.
860
- 861 • Bioinformatics pipeline and analysis scripts are available at <https://github.com/oueme-fungi/oueme-fungi-transect>.
862

863 **Author Contributions**

864 Sampling was planned and carried out by BF, NSY, and MR. Bioinformatics and data analysis
865 were performed by BF with input from MB, AR, and MR. Scripts and R packages were
866 written by BF. The manuscript was drafted by BF and MR. All authors contributed to and
867 approved the final version of the manuscript.

868 **List of Figures**

869 1 Venn diagrams of shared ASVs and OTUs between different sequencing tech-
870 nologies 35

871 2 Comparison between read numbers for different sequencing strategies 36

872 3 Summary of taxonomic assignments 37

873 4 Taxonomic composition of fungal community at the class level 38

874 5 Distance-decay plot for community dissimilarities and spatio-temporal distance 39

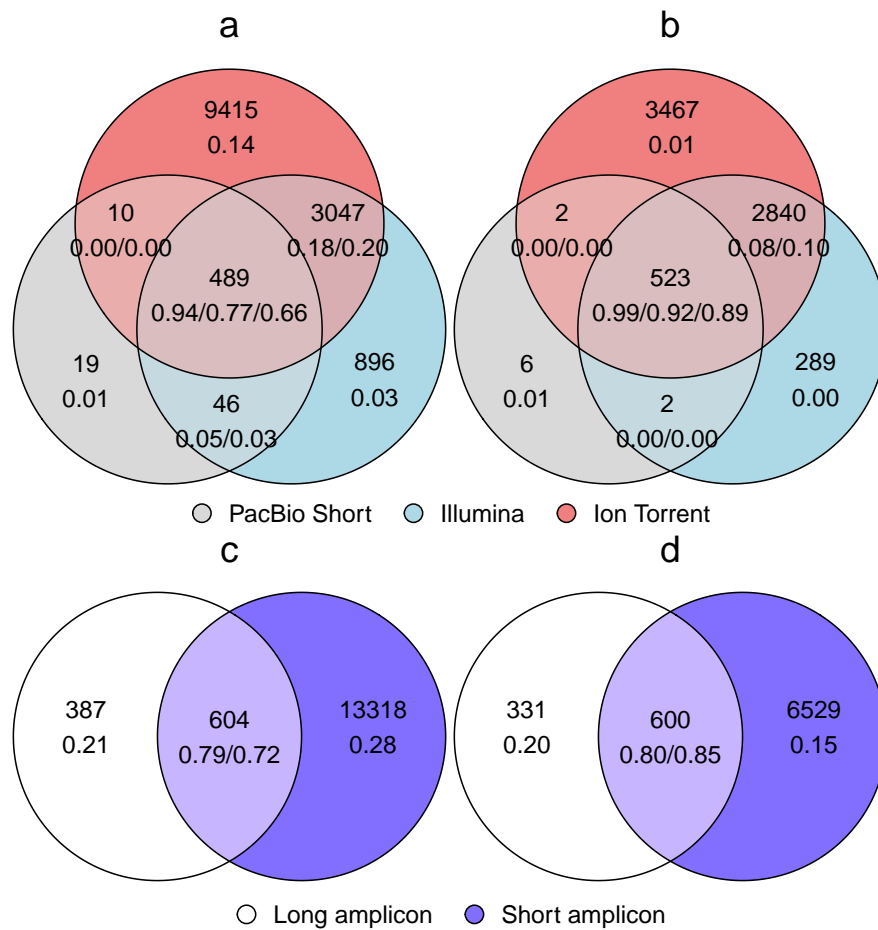


Figure 1: Venn diagrams showing shared ITS2-based ASVs (*a*, *c*) and 97% OTUs (*b*, *d*) between different sequencing technologies from the same short amplicon library (*a*, *b*), and between long and short amplicon libraries (*c*, *d*). In each region, the number of ASVs/OTUs is given above, while the fractions of reads for each sequencing strategy are shown below. For short amplicons in *c* and *d*, ASV/OTU counts reflect detection by any of the three technologies, and read counts represent the mean fraction of reads across the three technologies.

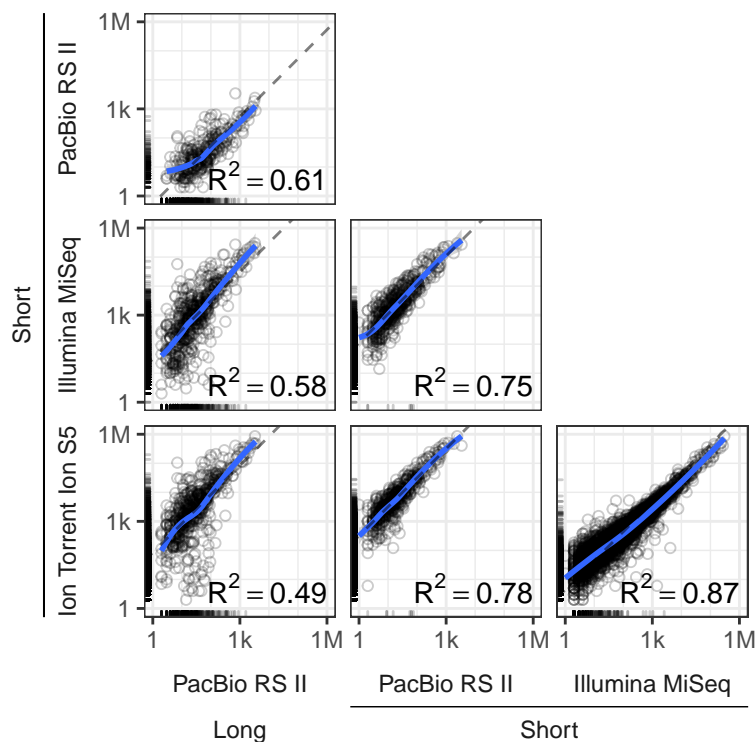
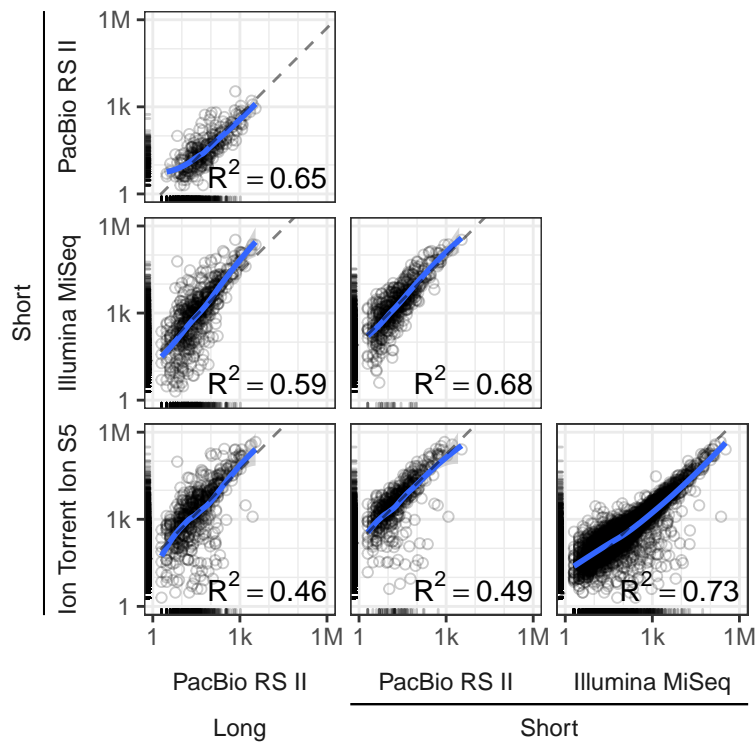


Figure 2: Comparison between read numbers for different sequencing strategies, by ASV (a) and 97% OTU (b). ASVs/OTUs which were detected by one sequencing strategy but not the other are plotted as tick marks along the axes. Dashed line represents a constant ratio of read numbers. The blue line is a LOESS smooth of the data, with associated uncertainty in grey shading. R^2 value displayed is for log-transformed non-zero read numbers. ³⁶

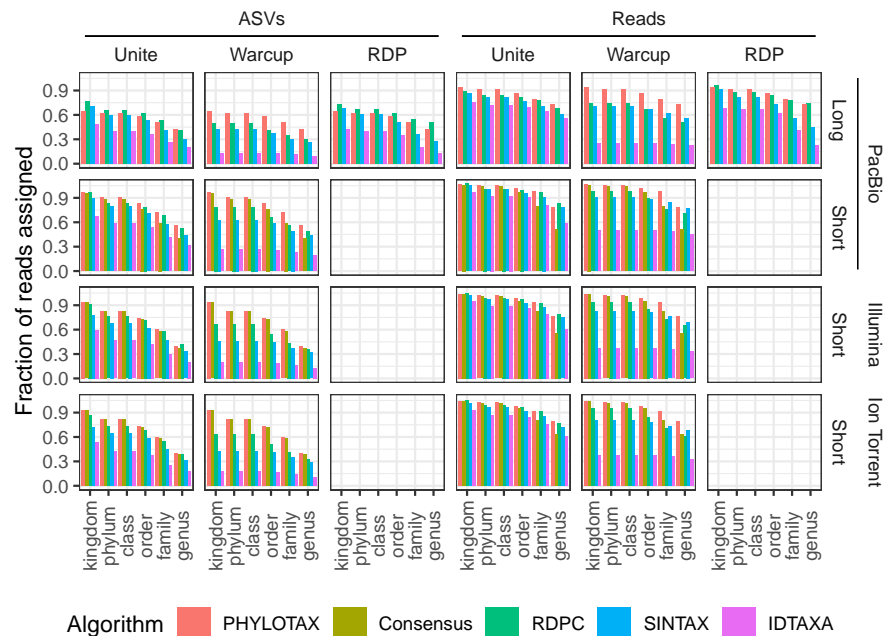


Figure 3: Fraction of ASVs (left) and reads (right) assigned to each taxonomic rank, for different sequencing technologies (PacBio RS II, Illumina MiSeq, Ion Torrent Ion S5), amplicons (Long, Short), reference databases (Unite, Warcup, RDP), and assignment algorithms (PHYLOTAX, Consensus, RDPC, SINTAX, IDTAXA). Consensus and PHYLOTAX assignments are based on the consensus of RDPC, SINTAX, and IDTAXA, using all available databases and, in the case of PHYLOTAX, phylogenetic information. These two methods are plotted in each column to compare with results for the individual databases.

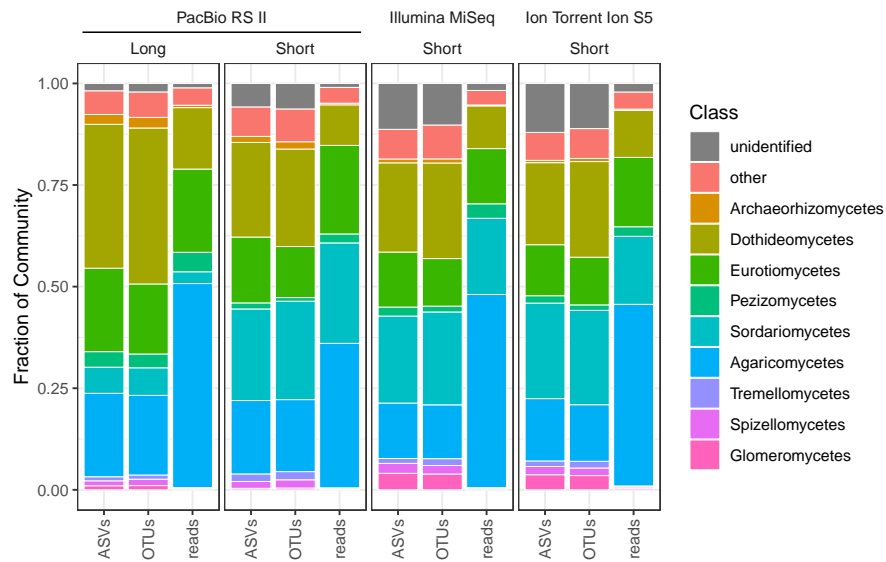


Figure 4: Taxonomic composition of fungal community at the class level. Values represent the fraction of all ASVs, OTUs, or reads which were assigned to kingdom Fungi. Assignments based on PHYLOTAX. Classes which represented less than 2% of reads, OTUs, and ASVs in all datasets are grouped together as “other”.

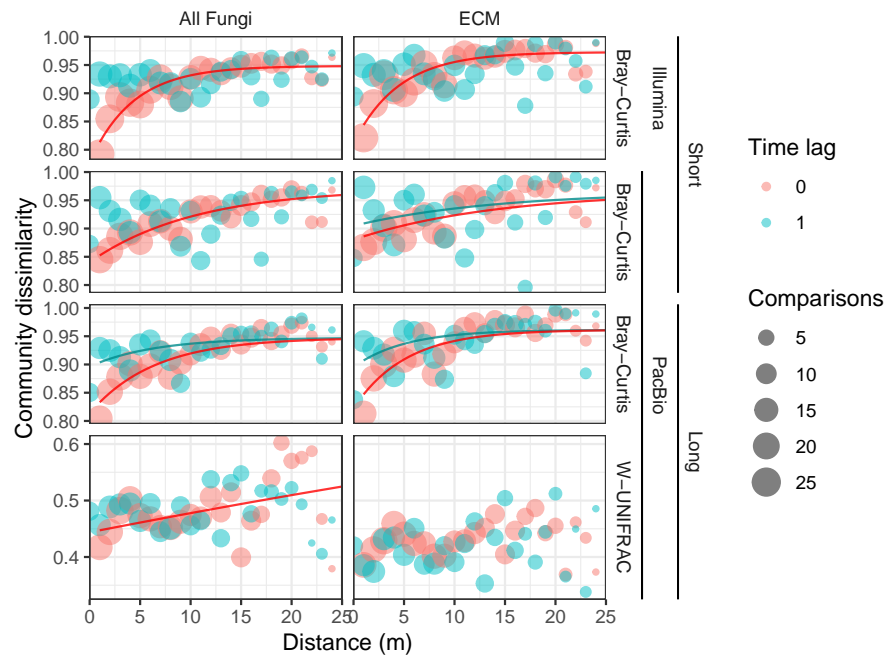


Figure 5: Distance-decay plot for community dissimilarities and spatio-temporal distance. Circles represent community data from short (top two rows) and long (bottom two rows) amplicon libraries, sequenced by Illumina MiSeq (top row) or PacBio RS II (bottom three rows). Community dissimilarities are calculated using the Bray-Curtis dissimilarity for all datasets (top three rows) and using the weighted UNIFRAC dissimilarity for the long amplicon library, for which a phylogenetic tree could be constructed (bottom row). The left column represents the full fungal community, and the right column only sequences identified as ECM. The color of each circle represents the time lag between samples being compared (0 or 1 year), and the size represents the number of comparisons for that spatial distance and time lag. Lines are the best-fit lines for an exponential decay to max model. The model was only fit for datasets where the Mantel test indicated a significant relationship between community dissimilarity and spatial (for the 0 year timelag) or spatiotemporal (for the 1 year time lag) distance.